Park, J., Stolle, C., Xiong, C., Lühr, H., Pfaff, R. F., Buchert, S., Martinis, C. R. (2015): A dayside plasma depletion observed at midlatitudes during quiet geomagnetic conditions. - *Geophysical Research Letters*, *42*, 4, p. 967-974.

DOI: http://doi.org/10.1002/2014GL062655

AGU PUBLICATIONS

Geophysical Research Letters

RESEARCH LETTER

10.1002/2014GL062655

Special Section:
ESA's Swarm Mission, One Year in Space

Key Points:
- Dayside plasma density depletion during a quiet time at low-altitude midlatitude ionospheric F-layer
- Dayside plasma density depletion elongated from northwest to southeast
- Dayside plasma density depletion without identifiable diamagnetic effect

Correspondence to:
J. Park,
park@gfz-potsdam.de

Citation:
Park, J., C. Stolle, C. Xiong, H. Lühr, R. F. Pfaff, S. Buchert, and C. R. Martinis (2015), A dayside plasma depletion observed at midlatitudes during quiet geomagnetic conditions, *Geophys. Res. Lett.*, *42*, 967–974, doi:10.1002/2014GL062655.

Received 2 DEC 2014
Accepted 16 JAN 2015
Accepted article online 24 JAN 2015
Published online 21 FEB 2015

A dayside plasma depletion observed at midlatitudes during quiet geomagnetic conditions

Jaeheung Park[1,2], Claudia Stolle[1,3], Chao Xiong[1], Hermann Lühr[1], Robert F. Pfaff[4], Stephan Buchert[5], and Carlos R. Martinis[6]

[1]Helmholtz Centre Potsdam, GFZ, German Research Centre for Geosciences, Potsdam, Germany, [2]Now at Korea Astronomy and Space Science Institute, Daejeon, South Korea, [3]Faculty of Science, University of Potsdam, Potsdam, Germany, [4]NASA Goddard Space Flight Center, Greenbelt, Maryland, USA, [5]Swedish Institute of Space Physics, Uppsala, Sweden, [6]Center for Space Physics, Boston University, Boston, Massachusetts, USA

Abstract In this study we investigate a dayside, midlatitude plasma depletion (DMLPD) encountered on 22 May 2014 by the Swarm and GRACE satellites, as well as ground-based instruments. The DMLPD was observed near Puerto Rico by Swarm near 10 LT under quiet geomagnetic conditions at altitudes of 475–520 km and magnetic latitudes of ~25°–30°. The DMLPD was also revealed in total electron content observations by the Saint Croix station and by the GRACE satellites (430 km) near 16 LT and near the same geographic location. The unique Swarm constellation enables the horizontal tilt of the DMLPD to be measured (35° clockwise from the geomagnetic east-west direction). Ground-based airglow images at Arecibo showed no evidence for plasma density depletions during the night prior to this dayside event. The C/NOFS equatorial satellite showed evidence for very modest plasma density depletions that had rotated into the morningside from nightside. However, the equatorial depletions do not appear related to the DMLPD, for which the magnetic apex height is about 2500 km. The origins of the DMLPD are unknown, but may be related to gravity waves.

1. Introduction

Equatorial plasma bubbles (EPBs) generally occur at night [e.g., *Woodman*, 2009], but their existence during daytime has been known for a long time. Ionograms obtained by the Alouette I satellite in 1968–1969 exhibited nonnegligible occurrences of dayside irregularities in the topside ionosphere [*Dyson*, 1977]. In situ plasma density measurements also demonstrated that EPBs can occur during daytime [e.g., *Burke et al.*, 1979; *Oya et al.*, 1986; *Oyama et al.*, 1988]. *Karpachev et al.* [2014] reported significant occurrences of daytime ionospheric ducts (or equivalently, ionospheric irregularities) in the topside ionograms obtained by Interkosmos-19.

Those statistical studies revealed that (1) dayside EPBs occur more frequently in the early morning than during noon/afternoon hours and (2) dayside EPBs generally occur at lower magnetic latitudes (MLAT) than nightside EPBs (afternoon: $\leq 20°$ and nightside: $\leq 30°$). *Li et al.* [2012] reported on a case where dayside EPBs were observed at $\geq 20°$ MLAT until 1015 in local time (LT) during magnetically disturbed conditions (minimum $D_{ST} = -149$ nT). An inverse relationship between MLAT and LT was suggested for dayside EPBs.

Woodman et al. [1985] reported two postnoon EPBs at the Jicamarca radar during geomagnetically quiet periods (the daily minimum $D_{ST} = -26$ nT on 26 March 1974 and -23 nT on 1 February 1984). Both events occurred only above 600 km altitude. *Chau and Woodman* [2001] reported one postnoon EPB at Jicamarca during a late recovery phase of a storm (the daily minimum $D_{ST} = -41$ nT on 11 April 2000). The dayside EPB was limited to altitudes above 950 km. *Huang et al.* [2013] reported two dayside EPBs encountered by the Communications/Navigation Outage Forecasting System (C/NOFS) satellite during moderate magnetic activity ($D_{ST} \geq -72$ nT). Both of the two EPBs were initiated before sunrise and observed above 600 km altitude after 09 LT. *Fukao et al.* [2003] observed a morning EPB in a low-latitude region (dip latitude ~10°) during a storm recovery phase (minimum $D_{ST} = -98$ nT). The EPB was initiated at a very low altitude of 200–250 km near sunrise and reached about 550 km altitude around 0700 LT, after which it disappeared.

Huang et al. [2013] suggested that dayside EPBs prefer higher altitudes since (1) dayside EPBs are remnant of nightside/presunrise ones and (2) EPBs at higher altitudes are better protected from active dayside photo-ionization and refilling. *Li et al.* [2012] suggested that geomagnetic disturbance creates favourable conditions for dayside EPBs. The disturbance dynamo *E* field and the negative ionospheric storm during a geomagnetic disturbance support the formation/persistence of dayside EPBs (e.g., to hinder EPB refilling).

To summarize, favorable conditions for occurrence of dayside EPBs have been suggested to be (1) at early morning LT, (2) at low latitude, (3) at high altitude, and (4) during geomagnetic disturbance. All case studies so far correspond to at least one of the four conditions, to the best of the authors' knowledge. Under quiet geomagnetic conditions no previous study ever confirmed that EPBs below 600 km altitude can persist beyond 0900 LT.

There are some other questions to be answered for dayside EPBs. First, it is unknown yet whether dayside EPBs exhibit hemispheric conjugacy. For most satellites used for previous studies on dayside EPBs, the inclination angles were low: 31° for Hinotori and 13° for C/NOFS. Second, it is unclear whether the dayside EPBs also exhibit inverted-C structures which are typical for nightside EPBs [e.g., *Kelley et al.*, 2003]. Previous studies on dayside EPBs mainly relied on single-satellite observations [e.g., *Huang et al.*, 2013] or ground-based observations [e.g., *Woodman et al.*, 1985], neither of which is suitable for figuring out the large-scale horizontal geometry of dayside EPBs.

In comparison with reports of dayside EPBs, reports of in situ measurements of dayside, midlatitude plasma depletions (DMLPD) are even less common, except perhaps with respect to gravity waves (GWs) and dayside medium-scale traveling ionospheric irregularities [e.g., *Onishi et al.*, 2009]. In this paper we report observations of DMLPDs encountered by multiple satellites and ground-based instruments on 22 May 2014. We will demonstrate that these depletions are not likely associated with EPBs, but more likely represent a locally driven phenomenon in the midlatitude ionosphere.

2. Instruments and Data

The Swarm constellation consists of three identical satellites [*Friis-Christensen et al.*, 2008], which were launched on 22 November 2013 into a polar orbit (inclination angle ∼87.3°). Their orbits were progressively separated after launch, and the satellites reached the final constellation in mid-April 2014. The satellite pair at lower altitudes, Swarm-Alpha and Swarm-Charlie were approximately at 475 km altitudes in May 2014 flying side by side with a longitudinal separation of about 1.5° at the equator. The along-track (approximately north-south) separation of this pair was about 9 s: 7.5 km/s × 9 s = 68 km. Swarm-Bravo is located at an altitude higher by about 50 km than the satellite pair, Swarm-Alpha and Swarm-Charlie. Each Swarm satellite carries a Langmuir Probe (LP) to measure electron density (n_e) and temperature (T_e) twice a second. Ongoing validation studies suggest that T_e is somewhat higher than expected, but relative variations of T_e can be trusted. The dual-frequency receiver of the Global Navigation Satellite System (GNSS) signals is used to calculate total electron content (TEC) between Swarm and the GNSS satellites. Geomagnetic field vectors are measured by a Vector Fluxgate Magnetometer and an Absolute Scalar Magnetometer at the nominal data rate of 1 Hz.

The Gravity Recovery and Climate Experiment (GRACE) mission consists of two identical satellites separated by about 220 km [*Tapley et al.*, 2004]. The mission currently operates in a polar orbit at altitudes of about 430 km, which is slightly lower than those of Swarm. The communication link between the two GRACE satellites is used to estimate TEC in between, which yields in situ ionospheric n_e when divided by the intersatellite distance [see *Xiong et al.*, 2010].

C/NOFS [*de La Beaujardière et al.*, 2009] was launched into an elliptical orbit of 400 × 850 km altitudes with orbit inclination angle of ∼13°, equipped with various instruments designed to measure n_e as well as other parameters such as *E* field and ion drift velocity. Boston University operates a multispectral airglow camera at Arecibo. GNSS receivers in Saint Croix (Virgin Islands) and Bermuda are used to generate ground-based TEC data. For details of the ground-based instruments, readers are referred to *Martinis and Mendillo* [2007].

3. Observations

We investigate a DMLPD which was observed on 22 May 2014. The day was characterized by extremely low geomagnetic activity: throughout 13–22 May 2014 the minimum D_{ST} index was −15 nT. The minimum *AL* index was −179 nT from 13 May until 1400 in universal time (UT) on 22 May 2014, when the DMLPD was first

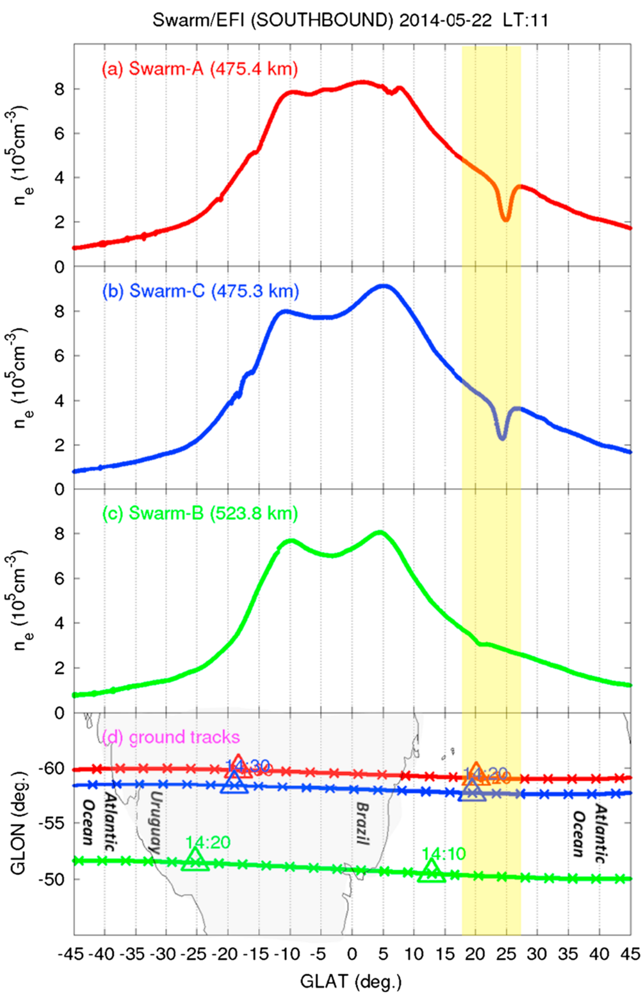

Figure 1. Profiles of n_e observed by Swarm/LP: (a) Swarm-Alpha, (b) Swarm-Charlie, and (c) Swarm-Bravo. (d) Orbital tracks on a geographic map rotated clockwise by 90°N with the same color as used for Figures 1a–1c.

encountered by Swarm. The $F_{10.7}$ ($P_{10.7}$) index and the maximum K_p index were 114.1 (129.7) and 3.3 on this day, respectively.

Figures 1a–1c show n_e profiles observed by the three Swarm satellites. Figure 1d presents the geographic location of the spacecraft (see the caption for details). Around 25°N in geographic latitude (GLAT) Swarm-Alpha and Swarm-Charlie encountered a DMLPD around 60°W in geographic longitude (GLON). The DMLPD location is at 475 km above the Atlantic Ocean to the northeast of Puerto Rico, corresponding to approximately 30°N MLAT and 1030 LT. The western satellite (Swarm-Alpha) observed the DMLPD at higher GLAT than the eastern satellite (Swarm-Charlie). The DMLPDs observed by the satellite pair, Swarm-Alpha and Swarm-Charlie are separated by 0.44° in GLAT and 1.44° in GLON, and they occurred around 25°N GLAT (see Figure 1). The tilt angle can be calculated as $\tan^{-1}\left(\frac{0.44}{1.44\times\cos 25^\circ}\right)$, which yields a tilt by ~20° clockwise from the geographic east-west direction. With the declination angle of geomagnetic field lines of about −15°, the tilt angle of the dayside EPB is about 35° clockwise from the geomagnetic east-west direction.

Swarm-Bravo at ~525 km also detected a weak depletion, although about 12 min earlier and at slightly lower latitude (~20°N GLAT) than the lower altitude satellites. The DMLPD encounter by Swarm-Bravo was ~8° to the east of the westernmost satellite, Swarm-Alpha. The DMLPDs observed by all the Swarm satellites exhibit smooth density profiles without substructures. None of the three Swarm satellites observed any comparable DMLPD in the southern hemisphere. Swarm/TEC profiles (figure not shown) also exhibit clear depletions by about 10% at the location of n_e decrease as shown in Figure 1, which confirms the Swarm/LP data.

Figure 2 presents (a) n_e, (b) T_e, and (c) $n_e \times T_e$, respectively. For both satellites the T_e inside the DMLPDs is higher than the ambient values by ~700 K. Although not shown in the figure, the DMLPD observed by Swarm-Bravo also exhibits T_e enhancement of ~70 K. The DMLPD at the Swarm-Alpha location is deeper and hotter than that in Swarm-Charlie while the two satellites were at similar altitudes. The maximum T_e inside the DMLPDs is about 10% higher for Swarm-Alpha than for Swarm-Charlie. On the contrary, the minimum n_e inside the DMLPDs is 2.07×10^{11} m^{-3} for Swarm-Alpha and 2.28×10^{11} m^{-3} for Swarm-Charlie (difference ~7.9%). The product of the n_e and T_e can represent electron energy density (or pressure P_e) [e.g., *Oyama et al.*, 1988], which is shown in Figure 2c. The minimum P_e for Swarm-Alpha (8.4 nPa) agrees with that for Swarm-Charlie (8.6 nPa) within 2%. The latitudinal profile of P_e exhibits depletion of about 15% inside the DMLPD.

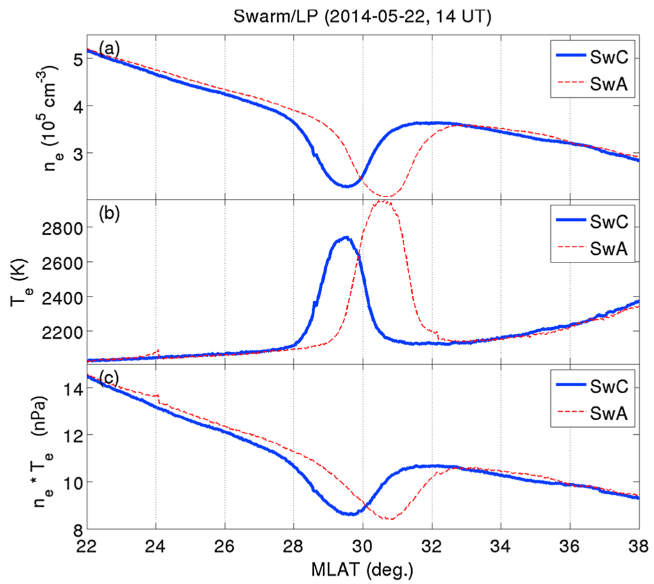

Figure 2. Latitudinal profiles of (a) n_e, (b) T_e, and (c) $n_e \times T_e$ in the vicinity of the dayside plasma density depletion.

Figure 3a presents n_e measured by GRACE at ~ 430 km at ~ 64°W. GRACE encountered a very modest plasma depletion near the same location as those observed by Swarm, but at ~20 UT (~16 LT) or ~6 h later than those of Figure 1. To identify DMLPDs from Figure 3a, we have first removed the large-scale variation, which is estimated by applying a Savitzky-Golay filter. The high-pass cutoff period is 31 s. By calculating the absolute value of the residuals we get the n_e fluctuation levels as shown in Figure 3b. We can identify significant fluctuations around 25° MLAT as in Figures 1 and 2 (e.g., 28–32° MLAT for Swarm-Alpha).

Figures 3c and 3d show TEC observation of a GNSS station at Saint Croix. Around 14 UT (i.e., near the time of Swarm DMLPD encounter in Figure 1) the vertical TEC exhibits a prominent dip near 20°N GLAT and 303°E (57°W) GLON. The magnitude of TEC decrease is about 2 total electron content unit (1 TECU = 10^{16} el m^{-2}), ~15% of the background. The Bermuda GNSS station also observed TEC depletions at similar geographic locations (figure not shown). Time-derivatives of TEC (i.e., GNSS phase fluctuations) at both stations were much smaller than we typically get from nightside irregularities (figure not shown).

4. Discussion

4.1. Space Environment Conditions

For the DMLPD event under study, the geomagnetic activity was very low, which does not support the connection of the DMLPD with the disturbance dynamo *E* field or a negative ionospheric storm [e.g., *Li et al.*, 2012]. The longitude and season of the event (~60°W in May) is unfavorable for nightside EPB occurrence [e.g., *Stolle et al.*, 2008]. The latitude of the event (~30°N MLAT) is also higher than those of

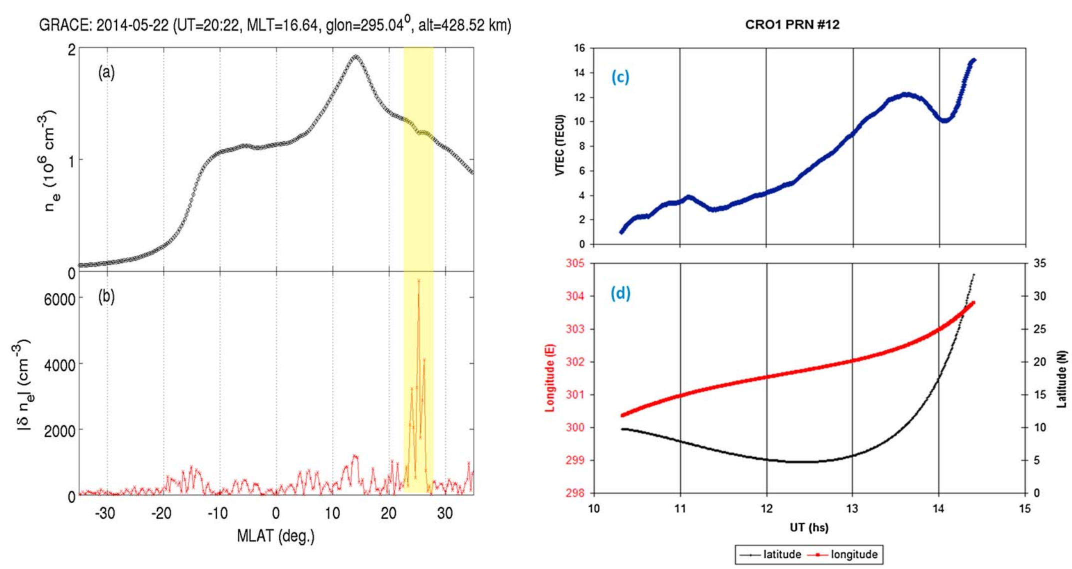

Figure 3. (left) n_e measured by GRACE around 64°W GLON: (a) in situ n_e and (b) n_e variations obtained by high-pass filtering and rectifying; (right) vertical TEC above the Saint Croix GPS station (Virgin Islands) on 22 May 2014: (c) vertical TEC and (d) subionospheric track coordinates at 350 km altitude.

quiet time nightside EPBs around the Swarm observation altitude [*Xiong et al.*, 2010]. Hence, the DMLPD under study is unlikely to be remnants of nightside EPBs [e.g., *Huang et al.*, 2013]. The altitude and time of the DMLPD encounter by GRACE (~430 km and ~16 LT) are outside the range where previous studies have reported dayside EPBs (see section 1).

We examined the plasma conditions during the morning LT in order to determine if the fountain effect might have been enhanced. Neither the in situ density nor ground-based TEC measurements showed any indication of enhanced Appleton anomaly. We also examined the limited *E* fields available from C/NOFS and did not see any enhanced zonal *E* fields. Thus, in concert with the very quiet conditions, we do not observe any near-dawn increase in the fountain effect dynamics that might have contributed to the generation of the DMLPD.

4.2. Initiation Time of the DMLPD

In order to investigate whether the DMLPD in our study originated before or after sunrise, we have checked observations by other ground-based instruments and satellites. At the Arecibo observatory (18.3°N, 66.7°W, 28°N MLAT) an airglow camera conducted uninterrupted observations on 22 May 2014, albeit only until local sunrise (~10 UT: ~4 h before the Swarm observations). The eastern edge of the camera field of view is around 60°W GLON, which overlaps with the DMLPD encounter by the lower Swarm pair. If the DMLPD was generated before sunrise, where plasma drift is eastward or nearly zero for this season and location [e.g., *Pacheco et al.*, 2011], the DMLPD should have been captured by the Arecibo camera. However, the Arecibo airglow images (figure not shown) exhibit no plasma irregularity signatures as strong as in Figure 1 (i.e., nearly 50% depletion from the background). We have further checked ground-based GNSS signals in the area and time of the 630.0 nm observations. Neither significant TEC changes nor phase fluctuations could be identified near Arecibo during nighttime, which also implies absence of nightside depletions.

4.3. Observations Near the Equator Gathered With the C/NOFS Satellite

Figure 4 shows stack plots of Vector Electric Field Instrument (VEFI) - fixed-bias Langmuir probe (LP) plasma density (16 Hz) for successive C/NOFS orbits on 22 May 2014 (refer to the caption for details). The region between 290° and 310°E GLON is highlighted by yellow shading (hereafter, "longitude of interest" or LOI), where Swarm and GRACE encountered the DMLPDs in the northern hemisphere. Because of the large declination of the magnetic field in this region (~−15°), the GLONs where the magnetic field lines intersect the DMLPDs reported here would actually be further to the east of the LOI. Also, the apex height of these magnetic field lines correspond to altitudes near 2500 km at the equator. It is nevertheless interesting to inspect the C/NOFS observations at the same LTs and GLONs where the DMLPD was encountered by Swarm.

During Orbit 33,283 (top frame) C/NOFS was on the nightside around the LOI and encountered no EPB. This observation is consistent with the lack of plasma depletions observed in the airglow instrument at Arecibo reported above. During the next orbit (Orbit 33,284), when C/NOFS was under daylight around the LOI, narrow (~20–40 km wide) and spiky EPBs were observed. Note that on the preceding orbit (33,283), C/NOFS was ~100 km lower in altitude and further to the north at the longitudes where these depletions were detected along orbit 33,284, so the satellite might have missed these higher-altitude depletions had they existed at nearby longitudes during the predawn period encountered on the previous orbit. Close inspection of the signatures of the very small plasma depletions in this region during the next several orbits as observed in the postsunrise period suggests that these depletions likely corresponded to ones that had existed at earlier LTs on preceding orbits and from which their deduced zonal velocities were very small.

The C/NOFS observations of morningside plasma depletions display characteristics consistent with postmidnight spread *F* plasma depletions that had rotated with the Earth into the postsunrise LTs. The morningside depletions observed in the C/NOFS data display substructures within the depletions, which are better seen with the higher sample rate data (not shown). These irregularities are inconsistent with the smooth density profiles associated with the DMLPDs in Figures 1–3. We conclude that the small, narrow EPBs evident in the C/NOFS morningside orbits on 22 May 2014 are not related in any direct fashion with the broader DMLPDs in Figures 1–3.

4.4. Remarks on Lack of Conjugacy

According to Figure 1, all three Swarm satellites observed DMLPDs in the northern hemisphere. Conversely, no Swarm satellite encountered a DMLPD at comparable latitudes in the southern hemisphere. GRACE observations revealed similar hemispheric asymmetry. Though the Swarm and GRACE orbits were not field

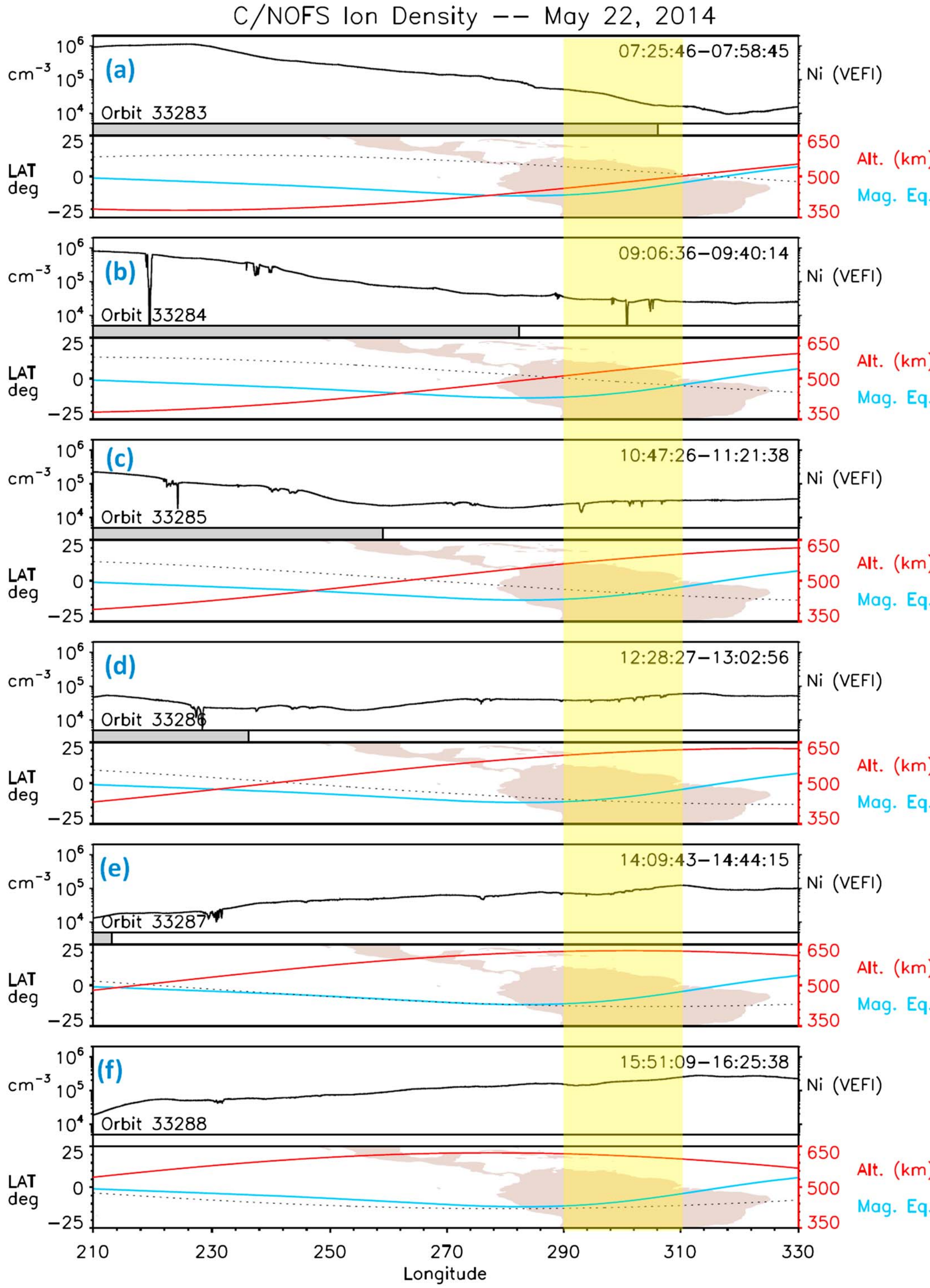

Figure 4. Stack plots of C/NOFS n_e on 22 May 2014. (a–f) Each frame corresponds to one orbit. The top presents n_e, and the bottom shows ground track of the satellite (black dotted line), satellite altitude (red), and location of the dip equator (blue). The black and white horizontal bars separating the upper and lower panels represent nightside and dayside locations, respectively.

aligned (magnetic declination angle at the DMLPD location ∼−15°), the lack of any DMLPD observed in the southern hemisphere is at least consistent with the supposition that they are local phenomena without conjugate counterparts.

4.5. Plasma Temperature Observations and Diamagnetic Effect

The T_e shown in Figure 2 is higher inside than outside the DMLPD, which is consistent with enhanced temperatures within dayside EPBs reported by *Oyama et al.* [1988] and *Huang et al.* [2013]. The enhanced plasma temperature of dayside EPBs has been attributed to active photoelectron heating applied to a limited number of charged particles, similar to the mechanism of the T_e morning overshoot [e.g., *Stolle et al.*, 2011], and similar processes may be at work in the DMLPDs. The enhanced temperature compensates for the n_e depletion, and largely equalize P_e ($= n_e \times T_e$) across DMLPD walls. The weak reduction of P_e within DMLPDs (Figure 2) is expected to result in only weak diamagnetic enhancements [e.g., *Lühr et al.*, 2003]. In Swarm magnetic field data (figure not shown) we could not identify conspicuous diamagnetic enhancement associated with the DMLPD.

4.6. Interpretation

At first glance, we consider interpreting these DMLPDs as extensions of the elongated EPBs found near the magnetic equator, particularly since the equatorial C/NOFS satellite observed extremely modest depletions that had rotated from the nightside into the morning sector. However, the magnetic apex height of the magnetic field lines that connect the location of the DMLPDs is 2500 km with no evidence of significant EPBs (in size, velocity, or altitude) that may have contributed to this extremely long range flux tube connection. Equatorial depleted flux tubes known to map to the midlatitudes have only been detected during times of strong magnetic storms when the *F* region plasma has been lifted considerably [e.g., *Pfaff et al.*, 2008], while the geomagnetic conditions present for the observations reported here were quiet.

Another consideration is that the distinctive tilt might be related to the “inverted-C” signature of EPBs that extend poleward. This shape is believed to be formed due to shear in zonal drifts with latitude of elongated interhemispherical depleted flux tubes [e.g., *Kelley et al.*, 2003]. This explanation is unlikely as the zonal drifts would be expected to have reversed directions in the morning compared to the evening [e.g., *Pacheco et al.*, 2011].

We thus must explore other explanations to understand these DMLPDs. One plausible explanation is that these features correspond to GWs. Future analysis, perhaps with the thermal ion imager on Swarm, may elucidate the processes at work.

5. Conclusions

In this study we have investigated an unusual DMLPD encountered on 22 May 2014 by the Swarm constellation and GRACE, satellites, as well as ground-based instruments. Notable findings of our study can be summarized as follows:

1. The DMLPDs were observed during quiet geomagnetic condition at altitudes near 430–520 km and at 25–30° MLAT over a duration extending from 10–16 LT. To our knowledge, no such dayside plasma structures have been reported under those conditions at midlatitudes.
2. The pair of depletions observed at 475 km near 30° MLAT were remarkably similar, even though they were separated by ∼1.4°E (150 km horizontal zonal separation). Each showed a very smooth, symmetric (with latitude) plasma density and electron temperature profile, without fine structures.
3. The formation flight of the Swarm-A and Swarm-C satellites demonstrates that the DMLPD is elongated from northwest to southeast in the northern hemisphere (tilt angle∼ 35° clockwise from the geomagnetic east-west direction). No similar plasma structures were observed in the southern hemisphere at midlatitudes.
4. We could not identify conspicuous diamagnetic enhancement of the in situ magnetic field within the DMLPDs. This is partly explained by the enhanced T_e within the depletions, which can compensate for n_e depletion and balance P_e across the depletion walls.

This study leaves several unanswered questions about DMLPDs. What is the key mechanism of the long-lasting DMLPDs during geomagnetically quiet times? Also, how can we explain the horizontal DMLPDs tilt? Exploiting the full capability of the Swarm payloads in constellation and additional diagnostics, we expect a significant step forward in understanding these features in terms of ionospheric physics.

Acknowledgments

The authors gratefully acknowledge OMNI data obtained from the GSFC/SPDF OMNI Web interface at http://omniweb.gsfc.nasa.gov. The Swarm data have been provided under the ESA/ESTEC contract 4000102140/10/NL/JA. We acknowledge the use of GRACE and C/NOFS data. The GRACE data have been provided after requests to GFZ. The Communication/Navigation Outage Forecast System (C/NOFS) mission, conceived and developed by the Air Force Research Laboratory, is sponsored and executed by the USAF Space Test Program. The Arecibo airglow images are available at http://www.buimaging.com. The ground-based GNSS observation data have been downloaded from the IGS SOPAC website. J. Park was partially supported by the "Planetary system research for space exploration" project, the basic research funding from KASI, and the Air Force Research Laboratory, under agreement FA2386-14-1-4004.

The Editor thanks two anonymous reviewers for their assistance in evaluating this paper.

References

Burke, W., R. Sagalyn, R. Rastogi, M. Ahmed, F. Rich, D. Donatelli, and P. Wildman (1979), Postsunrise refilling of the low-latitude topside ionosphere, *J. Geophys. Res.*, *84*(A8), 4201–4206, doi:10.1029/JA084iA08p04201.

Chau, J. L., and R. F. Woodman (2001), Interferometric and dual beam observations of daytime Spread-F-like irregularities over Jicamarca, *Geophys. Res. Lett.*, *28*, 3581–3584, doi:10.1029/2001GL013404.

de La Beaujardière, O., et al. (2009), C/NOFS observations of deep plasma depletions at dawn, *Geophys. Res. Lett.*, *36*, L00C06, doi:10.1029/2009GL038884.

Dyson, P. L. (1977), Topside irregularities in the equatorial ionosphere, *J. Atmos. Terr. Phys.*, *39*, 1269–1275.

Friis-Christensen, E., H. Lühr, D. Knudsen, and R. Haagmans (2008), Swarm-An Earth observation mission investigating geospace, *Adv. Space Res.*, *41*, 210–216, doi:10.1016/j.asr.2006.10.008.

Fukao, S., Y. Ozawa, M. Yamamoto, and R. T. Tsunoda (2003), Altitude-extended equatorial spread F observed near sunrise terminator over Indonesia, *Geophys. Res. Lett.*, *30*(22), 2137, doi:10.1029/2003GL018383.

Huang, C.-S., O. de La Beaujardière, P. A. Roddy, D. E. Hunton, J. O. Ballenthin, and M. R. Hairston (2013), Long-lasting daytime equatorial plasma bubbles observed by the C/NOFS satellite, *J. Geophys. Res. Space Physics*, *118*, 2398–2408, doi:10.1002/jgra.50252.

Karpachev, A. T., G. A. Zhbankov, V. P. Kuleshova, and V. A. Telegin (2014), Guided radio-wave propagation in the equatorial ionosphere according to the topside sounding onboard Interkosmos-19, *J. Atmos. Terr. Phys.*, *121*, 89–97, doi:10.1016/j.jastp.2014.10.008.

Kelley, M. C., J. J. Makela, L. J. Paxton, F. Kamalabadi, J. M. Comberiate, and H. Kil (2003), The first coordinated ground- and space-based optical observations of equatorial plasma bubbles, *Geophys. Res. Lett.*, *30*(14), 1766, doi:10.1029/2003GL017301.

Li, J., G. Ma, T. Maruyama, and Z. Li (2012), Mid-latitude ionospheric irregularities persisting into late morning during the magnetic storm on 19 March 2001, *J. Geophys. Res.*, *117*, A08304, doi:10.1029/2012JA017626.

Lühr, H., M. Rother, S. Maus, W. Mai, and D. Cooke (2003), The diamagnetic effect of the equatorial Appleton anomaly: Its characteristics and impact on geomagnetic field modeling, *Geophys. Res. Lett.*, *30*(17), 1906, doi:10.1029/2003GL017407.

Martinis, C., and M. Mendillo (2007), Equatorial spread F-related airglow depletions at Arecibo and conjugate observations, *J. Geophys. Res.*, *112*, A10310, doi:10.1029/2007JA012403.

Onishi, T., T. Tsugawa, Y. Otsuka, J.-J. Berthelier, and J.-P. Lebreton (2009), First simultaneous observations of daytime MSTIDs over North America using GPS-TEC and DEMETER satellite data, *Geophys. Res. Lett.*, *36*, L11808, doi:10.1029/2009GL038156.

Oya, H., T. Takahashi, and S. Watanabe (1986), Observation of low latitude ionosphere by the impedance probe on board the Hinotori satellite, *J. Geomagn. Geoelec.*, *38*, 111–123.

Oyama, K.-I., K. Schlegel, and S. Watanabe (1988), Temperature structure of plasma bubbles in the low latitude ionosphere around 600 km altitude, *Planet. Space Sci.*, *36*(6), 553–567.

Pacheco, E. E., R. A. Heelis, and S.-Y. Su (2011), Superrotation of the ionosphere and quiet time zonal ion drifts at low and middle latitudes observed by Republic of China Satellite-1 (ROCSAT-1), *J. Geophys. Res.*, *116*, A11329, doi:10.1029/2011JA016786.

Pfaff, R. F., C. Liebrecht, J.-J. Berthelier, M. Malingre, M. Parrot, and J.-P. Lebreton (2008), DEMETER satellite observations of plasma irregularities in the topside ionosphere at low, middle, and sub-auroral latitudes and their dependence on magnetic storms, in *Mid-Latitude Ionospheric Dynamics and Disturbances*, edited by P. M. Kintner et al., AGU, Washington, D. C., doi:10.1029/181GM27.

Stolle, C., H. Lühr, and B. G. Fejer (2008), Relation between the occurrence rate of ESF and the equatorial vertical plasma drift velocity at sunset derived from global observations, *Ann. Geophys.*, *26*, 3979–3988, doi:10.5194/angeo-26-3979-2008.

Stolle, C., H. Liu, V. Truhlík, H. Lühr, and P. G. Richards (2011), Solar flux variation of the electron temperature morning overshoot in the equatorial F region, *J. Geophys. Res.*, *116*, A04308, doi:10.1029/2010JA016235.

Tapley, B. D., S. Bettadpur, M. Watkins, and C. Reigber (2004), The gravity recovery and climate experiment: Mission overview and early results, *Geophys. Res. Lett.*, *31*, L09607, doi:10.1029/2004GL019920.

Woodman, R. F. (2009), Spread F—an old equatorial aeronomy problem finally resolved?, *Ann. Geophys.*, *27*, 1915–1934, doi:10.5194/angeo-27-1915-2009.

Woodman, R. F., J. E. Pingree, and W. E. Swartz (1985), Spread-F-like irregularities observed by the Jicamarca radar during the day-time, *J. Atmos. Terr. Phys.*, *47*(8–10), 867–874.

Xiong, C., J. Park, H. Lühr, C. Stolle, and S. Y. Ma (2010), Comparing plasma bubble occurrence rates at CHAMP and GRACE altitudes during high and low solar activity, *Ann. Geophys.*, *28*, 1647–1658, doi:10.5194/angeo-28-1647-2010.